Synthesis of Mil-100(Fe)@Fe_3O_4 Composite using Zircon Mining Magnetic Waste as an Adsorbent for Methylene Blue Dye

Marvin Horale Pasaribu[1], Karelius Karelius[1], Eka Putra Ramdhani[2], Retno Agnestisia1, and Zimon Pereiz[1], Erwin Prasetya Toepak[1,]*

[1]Department of Chemistry, Faculty of Mathematics and Natural Sciences, Universitas Palangka Raya, Palangka Raya 73111, Indonesia

[2]Department of Chemistry Education, Faculty of Teacher Training and Education, Raja Ali Haji Maritime University, Jalan Politeknik Senggarang, Tanjung Pinang 29111, Indonesia

Abstract. The objectives of the present study are to synthesize MIL-100(Fe)@Fe_3O_4 composite and to clarify its ability as an adsorbent for methylene blue dye. The magnetite (Fe_3O_4) was synthesized using iron precursor from the zircon mining magnetic waste. The MIL-100(Fe) was composited with magnetite using a room-temperature in situ synthesis method. The MIL-100(Fe)@Fe_3O_4 composite obtained was then characterized using the Fourier transform infrared spectroscopy and X-ray diffraction. The synthesized MIL-100(Fe) and MIL-100(Fe)@Fe_3O_4 were then used to adsorb methylene blue dye from aqueous phase. The maximum methylene blue removal from both adsorbents was obtained at pH of 9. The adsorption kinetics showed that the adsorption followed a pseudo second-order kinetics model with the rate constant values for MIL-100(Fe) and MIL-100(Fe)@Fe_3O_4 were 1.012 x 10-2 and 3.963 x 10-2 g/mg.menit, respectively. The results also showed that the adsorption isotherm of MIL-100(Fe) and MIL-100(Fe)@Fe_3O_4 follows the Langmuir isotherm for adsorption capacities were 137.70 and 151.47 mg/g, respectively. The results indicate that the iron content in the zircon mining magnetic waste as precursor for synthesis MIL-100(Fe)@Fe3O4 composite can be employed as an excellent adsorbent for removal of methylene blue dye from aqueous phase.

*Corresponding author: toepakerwin@mipa.upr.ac.id

INTRODUCTION

MIL-100 (Fe) is a type of metal-organic framework that comprises iron ions and 1,3,5-benzene tricarboxylate (BTC) ligands connected by a covalent coordination bond [1]. Several studies report that the large surface area of MIL-100(Fe) makes it an ideal adsorbent for various contaminants in water, abundant active sites, adjustable pore size, and good stability in water [1]. The traditional method for synthesis of MIL-100(Fe) involves a hydrothermal method at high temperature with the use of Fe ions and trimesic acid (H_3BTC), along with the addition of hydrofluoric acid (HF), which causes corrosion. However, some researchers have recently developed a synthesis method of MIL-100(Fe) at room temperature and free HF. This method is considered more environmentally friendly and provides opportunities for large-scale production in industry.

To increase its effectiveness as an adsorbent, MIL-100(Fe) can be composited with magnetite (Fe_3O_4). This combination aims to provide magnetic properties to MIL-100(Fe). By providing the magnetic properties, the separation of MIL-100(Fe) from aqueous phase after the adsorption process can be conducted easily and quickly using an external magnetic field[1–3].

Zircon is a mineral that is widely used in various industrial applications, such as ceramics (55%), chemicals (18%), refractory materials (14%), metal casting (10%), and other industries (3%) [4–6]. Suseno (2015) also reported that Indonesia is one of the zircon minerals-producing countries, with a contribution of 4% [6]. The increasing market demand in recent years for zircon has resulted in a rapid increase in zircon mining activities in Indonesia. This activity causes the emergence of large amounts of waste in the ex-mining area. If the exploitation of zircon which produces large amounts of waste is not balanced with its handling, it can cause environmental pollution [7]. However, several studies have recently revealed that zircon waste contains valuable minerals that can be reused for various purposes [8-10].

Magnetite, hematite, ilmenite, and siderite are minerals from zircon mining waste that are considered valuable. This is because these minerals contain the iron (Fe) element, which is considered to be used as a precursor for the Fe_3O_4 synthesis, which in this research will be composited with MIL-100(Fe). Utilizing secondary sources of zircon mining waste is one effort to maximize its use and reduce the impact of risks arising from the accumulation of this waste in the environment [8]. Several studies report that valuable minerals containing the element iron (Fe) can be separated from other minerals in zircon mining waste by using differences in the magnetic properties of the minerals. In general, minerals that do not respond to magnetic fields are called non-magnetic minerals consisting of quartz, mica, corundum, gypsum, zircon, and feldspar. Meanwhile, minerals that respond to magnetic fields are magnetic minerals containing the Fe element, such as magnetite, hematite, ilmenite, and siderite [8–10]. Therefore, the objectives of the present study are to synthesize MIL-100(Fe)@Fe_3O_4 composite using zircon mining magnetic waste and to clarify its ability as an adsorbent for methylene blue dye.

MATERIALS AND METHODS

2.1 Instrumentation

The FTIR 8400S Shimadzu model and X-ray diffractometer (XRD, Philips X-Pert MPD) was used to characterize both MIL-100(Fe) and the MIL-100(Fe) @Fe_3O_4 composite. Whereas the methylene blue concentration was determined by UV-Vis spectrophotometer.

2.2 Materials

The materials employed in this research comprised waste generated from zircon mining, methylene blue (C.I. 52015; p.a., Merck), $FeSO_4.7H_2O$ (p.a., Merck), HCl (p.a., Merck), NH_4OH (p.a., Merck), H_3BTC (p.a., Merck), and aquadest.

2.3 Preparation of Zircon Mining Magnetic Waste

The waste sample obtained from zircon sand processing was exposed to an external magnetic field for separating zircon mining waste containing magnetic and non-magnetic minerals. The waste sample that responds to external magnets was then collected and sieved until it passes a 100 mesh sieve.

2.4 Synthesis of Fe_3O_4 from Magnetic Zircon Mining Waste

A total of 5 grams of waste samples obtained from the preparation results were added to 50 mL of HCl (~12 M) and stirred using a magnetic stirrer for 90 minutes at a temperature of 80°C. The solution was then filtered using ash-free filter paper twice. The filtrate obtained was then titrated with NH_4OH solution until the pH of the solution became 9 and form a black precipitate from Fe_3O_4. The formed precipitate was then washed using distilled water, separated using an external magnetic field and dried at 110 °C for 3 hours.

2.5 Synthesis of MIL-100(Fe) and MIL-100(Fe) @Fe_3O_4 Composite

The synthesis of MIL-100(Fe) and MIL-100(Fe)@Fe_3O_4 composite refers to research conducted by Tan and Foo (2021) with several modifications [11]. To produce MIL-100(Fe), the process began with dissolving 13.7 mmol of $FeSO_4.7H_2O$ in distilled water, creating solution A. Concurrently, 9.1 mmol of H_3BTC was dissolved in a 1 M NaOH solution with a concentration of 3 mmol, yielding solution B. Subsequently, solution A was slowly introduced into solution B while maintaining a stirring speed of 200 rpm using a magnetic stirrer, ensuring that all of solution A had reacted. After 24 hours, the reaction mixture was stirred continuously at a rate of 200 rpm at room temperature. During this time, the mixture's color changed from bluish green to brownish-orange gradually. Afterward, the solid was brought down to room temperature, washed with warm water and methanol, and dried at 60°C for 12 hours. Furthermore, the MIL-100(Fe)@Fe_3O_4 composite was synthesized by the same method as above. However, solution A contains Fe_3O_4 (12.5%; w/w) that dissolved in 0.1 M HCL and $FeSO_4.7H_2O$ (13.7 mmol).

2.6 Adsorption Study on Methylene Blue in the Aqueous Phase

The batch technique was mainly employed in the adsorption investigation of methylene blue dye by MIL-100(Fe) and MIL-100(Fe)@Fe_3O_4 composites. Various factors affecting the rate of the adsorption process were studied by altering the initial pH of the solution (ranging from 5 to 10), contact time (ranging from 20 to 120 minutes), and the initial concentration of methylene blue (ranging from 50 to 350 mg/L). These experiments were conducted in 100 ml Erlenmeyer flasks containing 50 ml of methylene blue solution and placed in a shaker at 100 rpm for a duration of 3 hours at room temperature. After adsorption, the methylene blue concentration in each sample was determined using a UV-Vis spectrophotometer.

The adsorption kinetics of methylene blue in an aqueous phase was determined by examining the kinetic parameters for the adsorption process in relation to contact time. The data that was collected

was then compared to both a first-order kinetics equation [12] and a pseudo-second-order kinetics equation [13]. To characterize and describe the experimental data regarding adsorption isotherms, the Freundlich and Langmuir models were employed in this study.

RESULTS AND DISCUSSION

3.1 Synthesis and characterization of Materials

The Fe_3O_4, MIL-100(Fe), and MIL-100(Fe)@Fe_3O_4 materials had been synthesized in this study. The Fe_3O_4, MIL-100(Fe), and MIL-100(Fe)@Fe_3O_4 materials had black, reddish-orange, light brown colours, respectively. The synthesized MIL-100(Fe)@Fe_3O_4 appears to have magnetic properties as indicated by its ability to respond to external magnetic fields (**Figure 1**).

(a) (b)

Figure 1. The synthesized MIL-100(Fe) (a), and MIL-100(Fe)@Fe_3O_4 (b) were exposed to an external magnetic field

An FTIR spectrometer was used to characterize Fe_3O_4, MIL-100(Fe), and MIL-100(Fe)@Fe_3O_4 to confirm their functional groups. **Figure 2** shows the infrared spectrum of these materials. According to the FTIR spectrum results, the Fe_3O_4 compound exhibited absorption peaks at wavenumbers of 538 cm^{-1} and 443 cm^{-1} (**Figure 2(a)**), which are indicative of the stretching vibrations associated with FeO on tetrahedral sites (Fe^{2+} O^{2-}) and FeO on octahedral sites (Fe^{3+} O^{2-}) respectively [14] . Furthermore, the MIL-100(Fe) spectrum in **Figure 2(b)** shows the absorption peak at the wavenumbers of 3447 cm^{-1}, which is the vibrational absorption of the O-H group that appears due to the presence of bound water and free water in the MIL-100(Fe) sample. The peak at wavenumber of 3447 cm^{-1} represents a stretching vibration of the C=O group. The peaks observed at 1449 cm^{-1} and 1382 cm^{-1} correspond to stretching vibrations of the O-C-O group, while the peaks at 760 cm^{-1} and 710 cm^{-1} represent bending vibrations of the C-H group within the benzene ring of H_3BTC. Moreover, there is a crest that is connected to the stretching vibration of Fe-O that happens at a wavelength of 460 cm^{-1} [15].

The FTIR spectrum of MIL-100@Fe_3O_4 has almost the same spectrum as the MIL-100(Fe) sample (**Figure 2(c)**). The new peaks at wave numbers 3434 cm^{-1}, 1627 cm^{-1}, 1445 cm^{-1}, 459 cm^{-1}, and 763 cm^{-1} are the absorption of stretching vibrations of O-H, C=O, O-C-O, Fe-O, and bending vibrations of C-H groups, respectively. The relatively low peak of the O-H group at 3434 cm^{-1}, as well as the increased peak of the Fe-O bond at 459 cm^{-1} in the spectrum of MIL-100@Fe_3O_4 indicate the

increased number of Fe-O bonds and reduced interaction with free water due to the addition of Fe_3O_4 in MIL-100 structure.

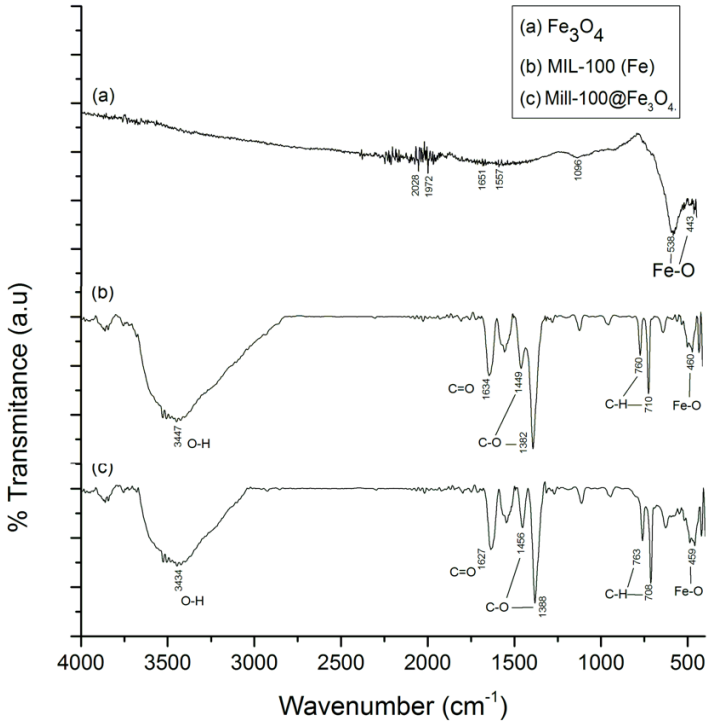

Figure 2. The FTIR spectra of Fe_3O_4 (a), MIL-100(Fe) (b), and MIL-100(Fe)@Fe_3O_4 (c)

The Fe_3O_4, MIL-100(Fe), and MIL-100(Fe)@Fe_3O_4 composite were successfully synthesized as comfirmed by XRD. **Figure 3** shows the X-ray diffractograms of Fe_3O_4, MIL-100(Fe), and the MIL-100(Fe)@Fe_3O_4 composite. In accordance with the standards established by the Joint Committee on Powder Diffraction (JCPDS; No. 19-629), it can be observed that the samples examined in this study exhibit characteristic peaks for iron oxide, specifically magnetite (Fe_3O_4), at 2θ angles of 30.143, 35.510, and 43.195, as depicted in **Figure 3(a)**. The X-ray diffractogram of the MIL-100(Fe) also has similar pattern to the previous research that used the synthesis methods at room temperature (CCDC No. 640536) at 2θ of 6.079; 10,217; 10,961; 12,486; 19,006; 20,035 ; 23,933 ; and 27,997 (**Figure 3(b)**). Moreover, it is worth noting that the diffractogram of the MIL-100(Fe)@Fe_3O_4 composite exhibited a strong resemblance to both MIL-100(Fe) (with peaks at 2θ angles of 10.07, 10.872, 19.958, 23.85, and 27.643) and Fe_3O_4 (with peaks at 2θ angles of 30.134, 35.389, and 43.164), as shown in **Figure 3(c)**.

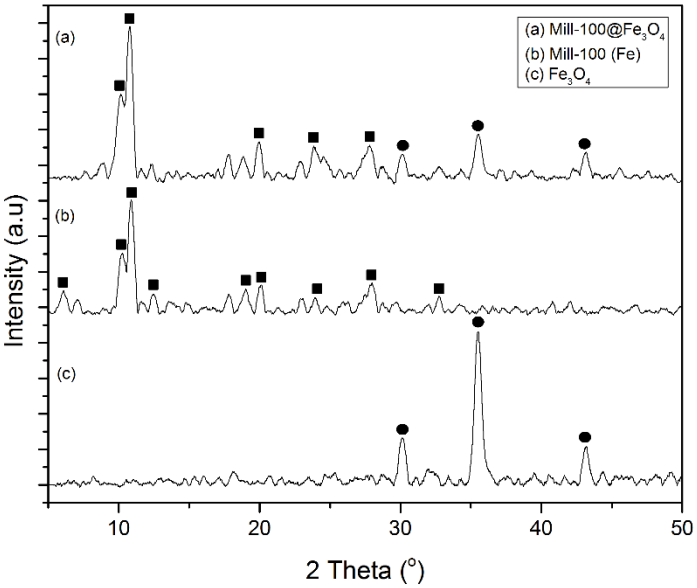

Figure 3. The XRD diffractograms of MIL-100(Fe)@Fe_3O_4 (a) MIL-100(Fe) (b), and Fe_3O_4 (c).

3.2 Adsorption results of Methylene Blue in the Aqueous Phase

Figure 4 illustrates the impact of pH on the adsorption capacity (qe) of both MIL-100(Fe) and the MIL-100(Fe)@Fe_3O_4 composite for methylene blue. The adsorption capabilities of both adsorbents are very similar, with the optimal pH for the adsorption process being pH 9. It was found that the sorption process by MIL-100(Fe) and the MIL-100(Fe)@Fe_3O_4 composite starts significantly when the pH is between 4 to 9. This is because at low pH (acidic conditions), the presence of protons from H^+ ions become more dominant, resulting in the active site of the carbonyl group on the surface of MIL-100(Fe) being protonated. This results in a reduced opportunity for cationic molecule of methylene blue to electrostatically interact with the active site of MIL-100(Fe). On the other hand, the active sites of MIL-100(Fe) tends to deprotonate at high pH (alkaline conditions). It causes the active sites of MIL-100(Fe) to be negatively charged, thus providing a greater opportunity for electrostatic interaction with cationic molecule of methylene blue. However, at pH > 9 (too alkaline conditions), the presence of OH^- ions becomes increasingly dominant, resulting in competition between OH^- ions and the active sites of MIL-100(Fe) electrostatically interacting with methylene blue. The same phenomenon was also demonstrated by MIL-100(Fe)@Fe_3O_4 composite.

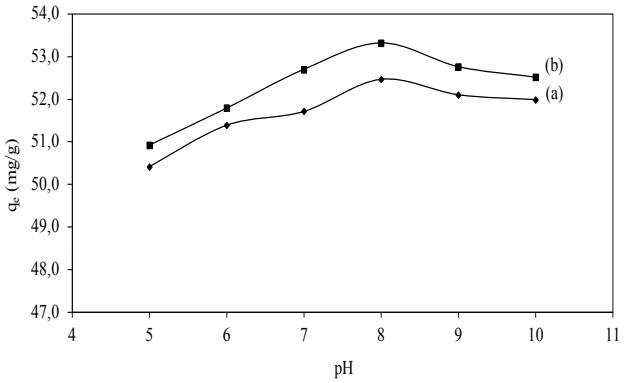

Figure 4. The effect of pH on adsorption capacity of MIL-100(Fe) (a) and MIL-100(Fe)@Fe_3O_4 (b)

The contact time effect on adsorption capacity (qe) of MIL-100(Fe) and MIL-100(Fe)@Fe_3O_4 composite on metylene blue can be seen in **Figure 5**. The results show that the adsorption of methylene blue on both adsorbents shows almost the same pattern. In addition, the results also show that adsorption of relatively large amounts of methylene blue occurs in the early minutes and and then tends to reach equilibrium.

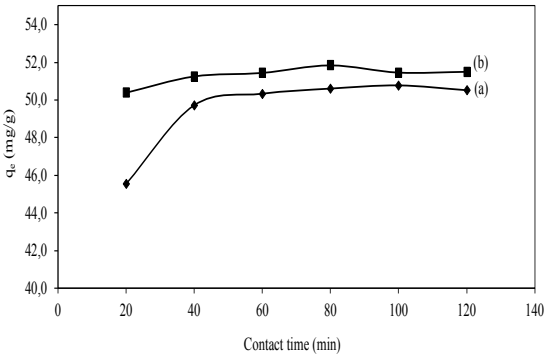

Figure 5. The effect of pH contact time on adsorption capacity of MIL-100(Fe) (a) and MIL-100(Fe)@Fe_3O_4 (b)

The data were then regressed against the first order kinetics and the pseudo-second-order kinetics equations (**Figure 6**). The correlation coefficient (R^2) was calculated from these plots to quantify the applicability of each model. The two models are suitable due to their linear characteristics. The outcome reveals that the correlation coefficient, which indicates the goodness of fit, strongly supports that the pseudo-second-order model ($R^2 > 0.999$) is a superior fit to the experimental data compared to the pseudo-first-order model ($R^2 > 0.700$).

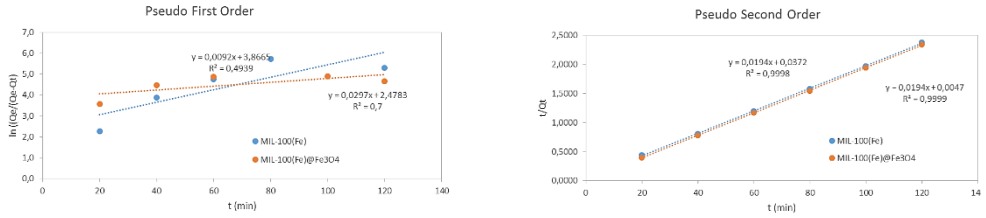

(a) (b)

Figure 6. Curves of pseudo first order kinetics (a) and pseudo second order kinetics (b) of methylene blue

This adsorption kinetics model shows that the adsorption rate is equivalent to the square of the methylene blue concentration, expressed by $(q_e-q_t)^2$ and indicates that the adsorption mechanism is chemisorptions. The outcome values of kinetic parameters are presented in **Table 1**.

Table 1. Adsorption kinetics models for methylene blue

Materials	Pseudo First Order		Pseudo Second Order	
	β (min^{-1})	R^2	k_2 (g/mg.min)	R^2
MIL-100(Fe)	0,0297	0,7000	1,012 x 10^{-2}	0,9998
MIL-100(Fe)@Fe_3O_4	0,0092	0,4939	3,964 x 10^{-2}	0,9999

The variation of methylene blue concentration effect on mg adsorption capacity of MIL-100(Fe) and MIL-100(Fe)@Fe_3O_4 composite can be seen in **Figure 7**. The results show that the adsorption of methylene blue on both adsorbents shows almost the same pattern. where both adsorbents have an optimum capacity at a methylene blue concentration of 250 ppm, which tends to reach equilibrium and then decreases with increasing concentration.

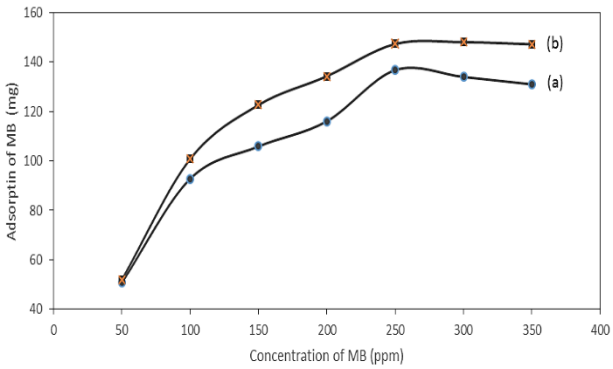

Figure 7. The effect of Methylene blue concentration on adsorption capacity of MIL-100(Fe) (a) and MIL-100(Fe)@Fe_3O_4 (b)

Adsorption equilibrium to determining isotherm patterns, adsorption capacity and adsorption energy. The connection between the quantity of

substances adsorbed onto the adsorbent and their equilibrium concentration is depicted in the isotherm pattern. The experimental data was analysed using two-parameter isotherm models, Langmuir and Freundlich, which gave further insight into the interaction between methylene blue and the solvent. **Figure 8** depicts the calculated results of the methylene blue absorption isotherm.

The correlation coefficient (R^2) was calculated from these plots to quantify the applicability of each model. The linearity of these plots indicates the applicability of the two models. The result indicates the correlation coefficient showing the Isotherm Langmuir model fits better the experimental data (R^2=0.9988) than Isotherm Freundlich model (R^2=0.9064).

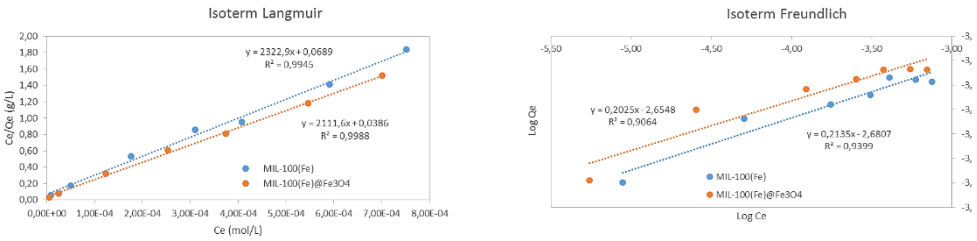

(a) (b)

Figure 8. Curves of Isoterm Langmuir model (a) and Isoterm Freundlich model (b) of methylene blue adsorption

The comparison of R^2 values shows that the equation in the Langmuir isotherm model has an R^2 value closer to 1, namely 0.993, so it can be concluded that the adsorption of methylene blue on MIL-100(Fe) and MIL-100(Fe)@Fe_3O_4 follows the Langmuir adsorption equation. Compliance with this model means that the adsorption of methylene blue on the adsorbent surface occurs through strong electrostatic interactions or chemisorption. The outcome values of equilibrium parameters of two isotherm models are presented in **Table 2**.

Table 2. Equilibrium kinetics models for methylene blue

Materials	Isoterm Langmuir				Isoterm Freundlich		
	B (mg/g)	K (L/mol)	E (kJ/mol)	R^2	B (mg/g)	N	R^2
MIL-100(Fe)	137.70	33663,77	25,74	0,9945	2,086 x 10^{-3}	4,684	0,9399
MIL-100(Fe)@Fe_3O_4	151.47	54563,31	26,93	0,9988	2,214 x 10^{-3}	4,938	0,9064

According to the Langmuir isotherm model, the adsorption capacity (B) of methylene blue on MIL-100(Fe) and MIL-100(Fe)@Fe_3O_4 can be determined, as presented in **Table 2**. MIL-100(Fe) exhibits an adsorption capacity (B) of 137.70 mg/g for methylene blue, while MIL-100(Fe)@Fe_3O_4 demonstrates a higher adsorption capacity (B) of 151.47 mg/g. The addition of Fe_3O_4 seems to influence the adsorption capability of MIL-100(Fe) for methylene blue, as suggested by this outcome. The application of the Langmuir isotherm model allows for the determination of the adsorption energy through the equation E = RT ln K. From the calculations, it is found that the energy required for the adsorption of methylene blue on MIL-100(Fe) and MIL-100(Fe)@Fe_3O_4 is 25.74 kJ/mol and 26.93

kJ/mol, respectively. This indicates that both adsorbents experience electrostatic interactions while sorption of methylene blue occurs. The electrostatic bonds are formed because the active sites of MIL-100(Fe) and Fe_3O_4 are negatively charged, while methylene blue has a positive charge, leading to attractive interactions between them.

CONCLUSION

Magnetite (Fe_3O_4) was successfully synthesized using iron precursors from zircon mining magnetic waste in this study. The obtained magnetite was then composited with MIL-100(Fe) using a room temperature in-situ synthesis method to form the MIL-100(Fe)@Fe_3O_4 composite which has magnetic properties. The synthesized MIL-100(Fe) and MIL-100(Fe)@Fe_3O_4 composites were employed for the removal of methylene blue from the aqueous phase using a batch system. Both adsorbents achieved their maximum dye removal efficiency at pH 9. The adsorption kinetics exhibited conformity with a pseudo-second-order kinetics model, with rate constant values of 1.01 x 10^{-2} g/mg.min for MIL-100(Fe) and 3.96 x 10^{-2} g/mg.min for MIL-100(Fe)@Fe_3O_4. The results also showed that the adsorption isotherm model of MIL-100(Fe) and MIL-100(Fe)@Fe_3O_4 follows the Langmuir isotherm for adsorption capacities were 137.70 and 151.47 mg/g, respectively. The findings suggest that the MIL-100(Fe)@Fe_3O_4 composite not only enhances its adsorption capacity for methylene blue but also enables the convenient separation of the adsorbent solid phase from the water phase with the aid of an external magnetic field.

CONFLICT OF INTEREST

The authors declare that there is no conflict of interest.

ACKNOWLEDGEMENTS

The author expresses gratitude to the Faculty of Mathematics and Natural Sciences at Universitas Palangka Raya for the research grant that was provided in 2023 under contract number 578/UN.24.10/PL/2023.

REFERENCES

1. L. Chen, C. H. Zhou, S. Fiore, D. S. Tong, H. Zhang, C. S. Li, S. F. Ji, and W. H. Yu, Appl Clay Sci **127–128**, 143 (2016)
2. I. M. Sadiana, K. Karelius, R. Agnestisia, and A. H. Fatah, Molekul **13**, 63 (2018)
3. K. Karelius, I. M. Sadiana, A. H. Fatah, and R. Agnestisia, Molekul **17**, 261 (2022)
4. *Beneficiation of Zircon Sand in South Africa H 2 SO 4 Dissolution of PDZ* (n.d.)
5. N. Hadi Haryanti, *UJI PASIR LIMBAH TAMBANG INTAN CEMPAKA* (n.d.)
6. T. SUSENO Puslitbang Teknologi Mineral dan Batubara Jalan Jenderal Sudirman, *Analisis Prospek Pasir Zirkon Indonesia Di Pasar Dunia, Triswan Suseno ANALISIS PROSPEK PASIR ZIRKON INDONESIA DI PASAR DUNIA Prospect Analysis of Indonesian Zircon Sand in the World Market* (2015)
7. W. Sun, B. Ji, S. A. Khoso, H. Tang, R. Liu, L. Wang, and Y.

Hu, Environmental Science and Pollution Research **25**, 33911 (2018)
8. I. Trisnawati, G. Prameswara, K. Rozana, H. Tri Murti Bayu Petrus, A. Prasetya, P. Mulyono, P. Sains dan Teknologi Akselerator, B. Jl Babarsari Kotak Pos, and ykbb Yogyakarta, *PELINDIAN ZIRKONIUM DARI TAILING MAGNETIK PASIR ZIRKON HASIL ROASTING MENGGUNAKAN NaOH* (2020)
9. A. Jordens, R. S. Sheridan, N. A. Rowson, and K. E. Waters, Miner Eng **62**, 9 (2014)
10. M. Pusat Teknologi Akselerator dan Proses Bahan-BATAN-Yogyakarta Jl Babarsari Nomor and K. pos, *PEMBUATAN KONSENTRAT ZIRKON DARI PASIR ZIRKON KALIMANTAN BARAT* (n.d.)
11. K. L. Tan and K. Y. Foo, Arabian Journal of Chemistry **14**, (2021)
12. R. L. Tseng, F. C. Wu, and R. S. Juang, J Taiwan Inst Chem Eng **41**, 661 (2010)
13. Y. S. Ho and G. Mckay, *Pseudo-Second Order Model for Sorption Processes* (1999)
14. V. Rathod, A. V. Anupama, R. V. Kumar, V. M. Jali, and B. Sahoo, Vib Spectrosc **92**, 267 (2017)
15. S. Huang, K. L. Yang, X. F. Liu, H. Pan, H. Zhang, and S. Yang, RSC Adv **7**, 5621 (2017)